Optics Communications 284 (2011) 201–206

Contents lists available at ScienceDirect

Optics Communications

journal homepage: www.elsevier.com/locate/optcom

Localization of light in evanescently coupled disordered waveguide lattices: Dependence on the input beam profile

Somnath Ghosh [a], G.P. Agrawal [b], B.P. Pal [a,*,1], R.K. Varshney [a]

[a] Physics Department, Indian Institute of Technology Delhi, Hauz Khas, New Delhi 110016, India
[b] Institute of Optics, University of Rochester, Rochester, NY 14627, USA

ARTICLE INFO

Article history:
Received 21 June 2010
Received in revised form 12 September 2010
Accepted 13 September 2010

Keywords:
Localization of light
Waveguide lattice
Refractive index perturbations
Disordered dielectric

ABSTRACT

We investigate how the transverse localization of light in evanescently coupled, disordered, lossless waveguide lattices depends on the shape and size of an input beam. Our detailed numerical study not only reveals waveguide-like propagation of the localized state inside such a disordered discrete medium but also shows that a specific localized state is independent of the spatial profile of the input beam. Dependence of the localized state on input beam parameters and lattice parameters is also reported. Our results should be of interest for engineering light propagation with discrete diffractive optics in practical optical geometries (e.g., microstructured arrays of optical waveguides, fiber arrays, etc.) and for realizing waveguide-like (without any diffractive spread) propagation even in the presence of structural disorders and refractive index perturbations.

1. Introduction

Sajeev John was the first to suggest theoretically that light might get localized in a disordered dielectric lattice structure [1], an effect analogous to the well-known phenomenon of Anderson localization [2] of an electronic wave packet. Raedt et al. [3] investigated the idea of light localization further and introduced the concept of transverse light localization in a semi-infinite disordered geometry i.e., confinement occurs only in the plane perpendicular to the direction of light transport. With the advent of and intense research on photonic bandgap devices and discrete photonic structures, transverse localization of light has attracted considerable attention in recent years in the context of disordered periodic structures [4–6]. In a 2007 experiment, Schwartz et al. [5] realized transverse localization of light in disordered, two-dimensional, photonic lattices and studied the interplay between a medium's nonlinearity and its degree of disorder. Lahini et al. [6] experimentally demonstrated the effect of a medium's nonlinearity on light localization and concluded that the nonlinearity in a disordered medium favors localization to occur within a shorter distance. The interplay between Anderson localization and the optical gain in a two-dimensional disordered medium has also been studied from the standpoint of realizing a random laser [7].

However, none of these studies seems to have considered the effect of input beam shape and size on the localization of light in a disordered dielectric medium. Further, study on dependence of the coupling efficiency into a localized state on spatial location of the input beam is missing in the literature. The absence of such a study, the ever-growing literature on light propagation in microstructured waveguide array devices and photonic crystals, and the possibility of light localization in disordered bandgap geometry [8] have motivated us to undertake the present investigation. In this paper, we report explicitly for the first time to our knowledge, dependence of the localized state on the shape and width of an optical beam when it is coupled into an evanescently coupled, disordered, waveguide lattice array. Our study reveals several underlying interesting features of light confinement to a localized state in such a medium of finite length. We have studied the nature of input light coupling to different localized modes of a disordered medium under different input excitation conditions. We also show that light can propagate without any diffractive spread (in the transverse direction) beyond the point of localization in a disordered lattice, a feature that mimics guided mode-like propagation. Our results should be useful for manipulating the flow of light in novel discrete photonic superstructures designed to exploit the Anderson type of light localization.

2. Simulation and methodology

Motivated by the experimental results reported in [5], we consider propagation of a continuous-wave (CW) beam in a lossless, disordered, dielectric structure. The medium's general refractive index n (x, y) is assumed to have a built-in periodicity in either of the two transverse directions and it alternates between n_1 and n_2

* Corresponding author. Tel.: +91 11 2659 1331; fax: +91 11 2658 1114.
E-mail address: bppal@physics.iitd.ernet.in (B.P. Pal).
[1] Currently on leave of absence from IIT Delhi as a Guest Scientist at Laboratoire de Physique de la Matière Condensée (LPMC), Universite de Nice Sophia Antipolis, CNRS UMR 6622, 06108 Nice Cedex 2, France.

0030-4018/$ – see front matter © 2010 Elsevier B.V. All rights reserved.
doi:10.1016/j.optcom.2010.09.032

along the x-direction, shown schematically in Fig. 1. In addition, it is assumed to vary randomly from these nominal values. For our study of light localization in such disordered media, we focus on an evanescently coupled, equally spaced, waveguide lattice [6] consisting of 100 unit cells. We assume that all the waveguides are buried inside a medium of constant refractive index n_0. The overall dielectric structure is homogeneous in the longitudinal z direction along which the optical beam is assumed to propagate. Such a structure should be realizable through the laser-inscripted waveguide fabrication technique [9,10] i.e. by inducing localized modifications of the material by shining a high intensity tightly focused laser beam (operating as CW or emitting femtosecond pulses) because it can increase the local refractive index of a transparent material such as glass. Typical refractive index changes Δn realizable by the laser-beam inscription technique are ~10^{-4} (for a CW beam) or ~0.001 (for a pulsed laser) [9]. In our numerical study, we have accordingly assumed the index contrast in the individual units of the lattice to be of this order. The disorderness in the chosen lattice geometry could result either from slight variations in the thickness of higher-index core layers, or in their spacing [6], or in their refractive indices. In this study, as a specimen, we consider randomness only in the refractive index of the chosen lattice.

In the paraxial limit, wave propagation inside a dielectric medium is, in general, governed by the following equation that is formally similar to the Schrödinger equation except that t is replaced by z [5]:

$$i\frac{\partial A}{\partial z} + \frac{1}{2k}\left(\frac{\partial^2 A}{\partial x^2} + \frac{\partial^2 A}{\partial y^2}\right) + \frac{k}{n_0}\Delta n(x,y)A = 0 \qquad (1)$$

where $A(r)$ is the electric-field amplitude of a CW optical beam, $E(r,t) = Re[A(r)e^{i(kz-\omega t)}]$. Here, $k = n_0\omega/c, n_0$ is the uniform background refractive index, and $\Delta n\ (x, y)$ represents a random deviation of the refractive index over its nominal value n_0. However, in our study we have considered 1D coupled waveguide lattice geometry. Thus, $\Delta n\ (x, y)$ is a function of x coordinate only. Accordingly, the transverse dependence of the field thus becomes a function of x alone. Because of the underlying periodic nature of the dielectric structure (see Fig. 1), $\Delta n(x)$ consists of a deterministic periodic part Δn_p of spatial period Λ and a spatially periodic random component δ (uniformly distributed over a specified range 0 to 1). Therefore, it can be algebraically expressed in the form

$$\Delta n(x) = \Delta n_p(1 + C\delta)H(x) \qquad (2)$$

where C is a dimensionless constant, whose value governs the level of disorder in the periodic backbone structure. The periodic function $H\ (x)$ takes the value 1 inside the higher-index regions and is zero otherwise.

We solve Eq. (1) numerically through the scalar beam propagation method, which we implemented in MatLab. We deliberately choose a relatively small refractive index contrast along with a relatively long unit-cell period compared to the wavelength ($\Lambda \gg \lambda$) to ensure that the

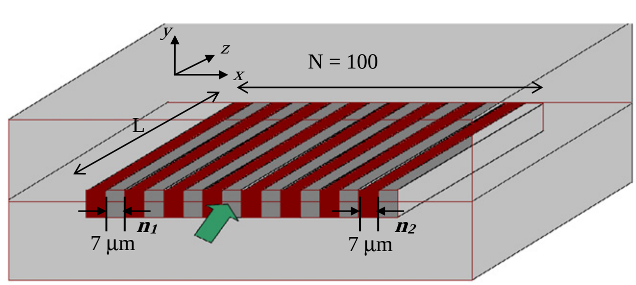

Fig. 1. Schematic of the chosen sample as evanescently coupled waveguides, each of equal width and spaced equally apart from its neighboring waveguide (100 unit cells); different shades of color signify different refractive indices over an average refractive index.

bandgap effects remain negligible. Every individual unit of the lattice functions as a single-mode waveguide at the operating wavelength λ when the lattice is perfectly ordered. We have also considered a sufficiently long sample length (>10,000λ) to seize the effect of linear discrete diffraction and to ensure that propagating light feels the existence of z-independent transverse disorder. We have chosen the aspect ratio of the lattice as well as the number of unit cells in such a way that any edge effects in the evolution of the beam could be easily avoided. Due to a finite width of our sample, there would always be a small but finite radiation loss; however, in our simulations, these small losses have been neglected. This is justified in practice if the number of unit cells is large and the geometrical aspect ratio is optimally chosen.

If M is the number of grid points along the x-direction, the disorderness of the medium is represented by an array of M random elements. This array is constructed using random numbers distributed uniformly in the range of 0 to 1. Since, scattering in a disordered system is of stochastic nature, we assign different random arrays for different realizations (chosen to be 100 in our numerical simulations) and average over 100 realizations of the lattice disorder.

3. Results

For simulating the waveguide lattice shown in Fig. 1, we have chosen a set of experimentally feasible parameters. We consider a waveguide array consisting of 100 evanescently coupled waveguides, each of 7 μm width and separated from each other by 7 μm (i.e., center-to-center spacing is 14 μm) whose length could vary from 5 to 20 mm. The lattice is buried within a background material of refractive index $n_0 = 1.46$. The value of Δn_p was chosen to be 0.001 i.e. the refractive index inside each waveguide is uniformly greater by this amount over its surroundings in the absence of disorder. To introduce disorder in the structure, we distribute the refractive index from one unit cell to the next in a random fashion following the prescription indicated in Eq. (2). An input CW beam at the operating wavelength of 980 nm is assumed incident on the unit cell located around the central region of our grid (irrespective of the index of the local lattice unit). The input beams were chosen to be either Gaussian, parabolic, hyperbolic secant, or exponential in shape. In all cases, irrespective of beam shapes, the input beam width (w_0) was set such that the full width at half maxima (FWHM) of the beam is 10 μm at the input plane of the sample. With this choice of width, the beam covers several high and low index sites at the input plane, and other initial conditions are not very critical to incorporate the diffraction effect [3].

We first consider the case of a perfectly periodic lattice (i.e. without any disorder) and set $C = 0$. Our chosen lattice geometry has already been exploited (either as a linear or as a nonlinear medium) to demonstrate discretization of light behavior [11–13] and confinement of light flow in weakly coupled waveguide arrays [14]. Because of the evanescent coupling among the waveguides, the beam initially spreads in the transverse direction and its power gets distributed across multiple lattice sites with propagation. We could observe such linear discrete diffraction effect [11] numerically with propagation of the light beam along our chosen 20 mm-long device as is evident from Fig. 2. A linear increase in the effective width of a beam along the sample length is known as the *ballistic mode* of light propagation [5]. From Fig. 2, this *ballistic mode* of beam propagation is clearly evident when a Gaussian beam is launched into the sample. A similar ballistic feature was seen if the input beam was chosen to be parabolic, hyperbolic secant, or exponential in shape. This discrete diffraction phenomenon could be observed irrespective of the point of incidence of the beam at the input plane of the lattice. Moreover, this feature was found to be independent of the characteristic size of the input beam. In other words it also did not depend whether the input beam covered one or more lattice sites.

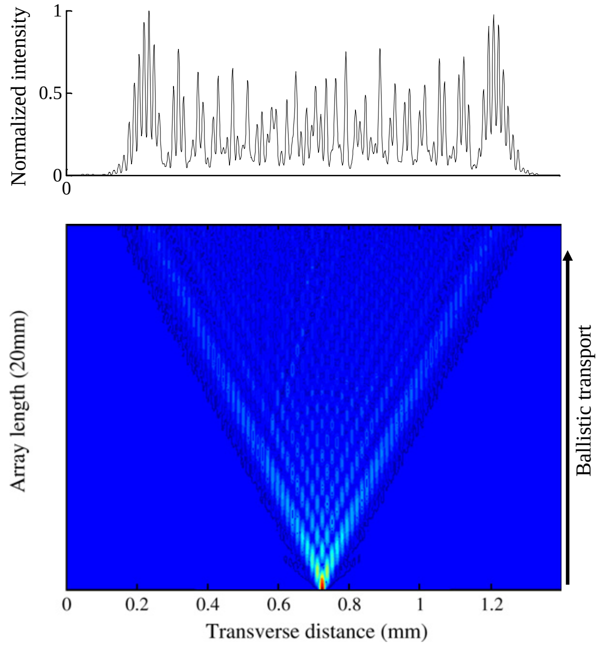

Fig. 2. Illustrative (contour plot) ballistic (discrete linear diffraction) mode of propagation of a Gaussian input beam of FWHM 6.75 μm (launched at the 52nd lattice site) through a 20 mm long perfectly ordered lattice. The calculated normalized intensity (diffracted) profile at the end of the waveguide lattice is also shown on the figure.

For studying propagation in a disordered medium, we repeat the preceding steps with the same set of parameters except for an additional parameter, namely the disorder parameter C, which was chosen at first to be as 0.2. The results are shown in Fig. 3, from which it can be seen that the presence of 20% disorder significantly modifies the propagation behavior of the beam as much as it opens up a waveguide-like channel through the lattice. The CW beam initially spreads in a ballistic fashion but soon its evolution is dictated by the transverse disorderness across its wings. When the beam width becomes comparable to the characteristic *localization length* [5] for the chosen level of disorder, the beam remains localized to the central region with further propagation beyond that point and acquires the exponential tail characteristic of light localization. Beyond the point of localization, fluctuations in the intensity become entirely statistical in nature. Physically, light scattered from disordered scattering centers interferes constructively and evolves toward a state whose envelope exhibits exponentially decaying tails that are the signature of a localized state [3,5], analogous to the Anderson localization of the electronic wave function. The presence of underlying periodicity enhances the interplay between scattering and constructive interference [8].

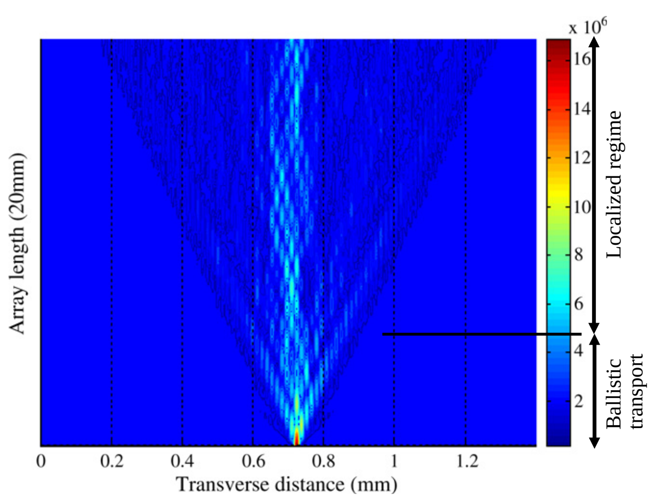

Fig. 3. Transition (contour plot) of an input Gaussian beam of FWHM 6.75 μm (launched at the 52nd lattice site) from ballistic regime to a localized regime while propagating through a 20 mm long 20% disordered waveguide lattice; the figure corresponds to a particular realization (i.e. a particular δ).

It is well known that transverse localization always occurs in a 1D disordered lattice which consists of infinite number of unit cells with any amount of disorder when the propagation distance is sufficiently long (similar to transverse localization in a 2D disordered lattice, but unlike the crucial requirement of a threshold strength of disorder for Anderson localization to occur in a 3D disordered system) [5,6]. However for a 1D disordered lattice with finite number of unit cells, the transverse localization of light is possible only for long enough distance of propagation of the beam through it. Thus in a disordered lattice of finite extent (which in our case consisted of 100 coupled waveguide units) the propagating light beam sees the initial ballistic expansion and then evolves to a state where ballistic and localized states co-exist [6]. If we increase the level of disorder in the lattice, the initial ballistic distance of propagation and consequential free diffraction-like broadening with propagation reduce and much faster transition to a localized state is achieved through a short intermediate mixed regime of ballistic and localized modes of propagation. Thus the interplay between sample aspect ratio and strength of disorder plays a key role to govern the propagation dynamics of the beam and the onset of the localized state in a finite lattice. In order to investigate this issue further, we study evolution of the beam through the lattice for different levels of disorder by varying the value of the C parameter in Eq. (2). To study the beam transport in more details, we checked the intensity distribution at the output end of the disordered lattices. For each value of C, we examined the output intensity distribution for several sample lengths in the range of 5 to 20 mm. To account for the statistical nature of the localization, we averaged the output intensity profile over 100 realizations (i.e., 100 different δ's). To highlight this statistical behavior over different realizations for a given level of disorder, we quantify the degree of localization through an *average effective width* (ω_{eff}) of the beam which is defined as [5]

$$\omega_{eff} = \langle P \rangle^{-1/2}$$

$$P \equiv \left[\int I(x,L)^2 \, dx \right] / \left[\int I(x,L) dx \right]^2$$

where P is averaged over multiple realizations of the same level of disorder. In Fig. 4a we depict the results of our study by plotting ω_{eff} of the output beam as a function of the sample length for different values of C (including $C=0$). In contrast to the case of a perfectly ordered lattice for which the effective beam width increases linearly with propagation (see case G which corresponds to $C=0$), this width increases sublinearly for a disordered lattice with finite values of C and saturates to a constant value, which corresponds to evolution to a localized light state when C exceeds a critical value ($C>40\%$). These results clearly demonstrate transition from a ballistic mode of propagation to a localized state in the presence of relatively strong disorder, which is required to observe localization for the particular lattice length. Fig. 4b reveals a clear statistical nature of the study showing the statistical standard deviation (error bars) along with the average value of the effective widths. In other figures, we have not shown the error bars just to avoid the possible reduction of clarity of the plot. In Fig. 5 we plot the ensemble-averaged output beam width as a function of the sample length for four different input spatial intensity profiles (parabolic, hyperbolic secant, and exponential along with Gaussian shape) for different levels of disorder. In other three cases, the CW beam exhibits a behavior that is qualitatively similar to that of a Gaussian beam in Fig. 4a. This similarity leads us to conclude that the phenomenon of light localization in a disordered waveguide

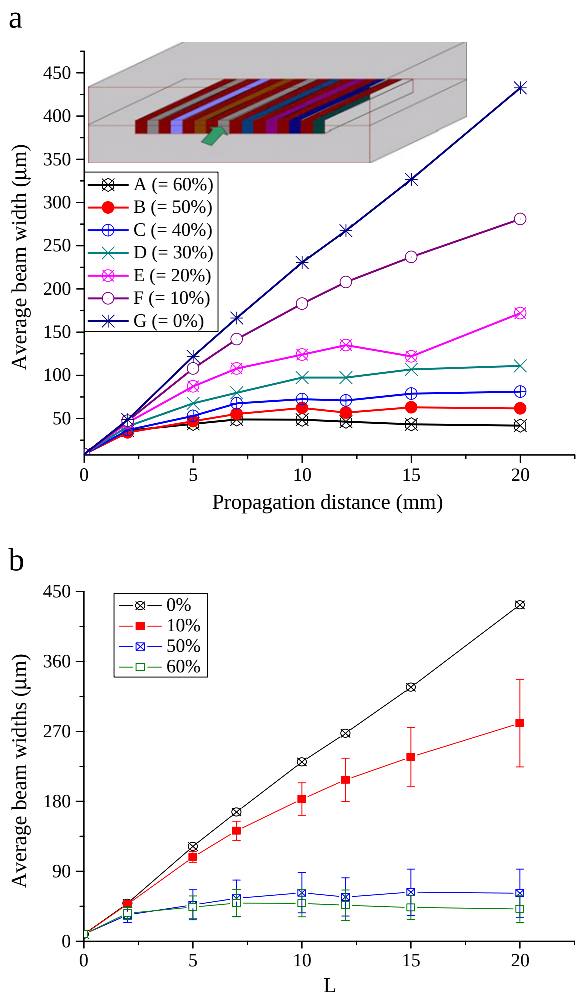

Fig. 4. a. Variation in the ensemble-averaged effective width (ω_{eff}) of a Gaussian beam (FWHM 10 µm) with propagation through the waveguide lattice for different strengths (C) of disorder labeled as A (=60%), B (=50%), C (=40%), D (=30%), E (=20%), F (=10%), and G (=0%). The inset shows schematic of the chosen disordered sample; different shades of color signify different refractive indices over an average index; in the calculations, the input beam was launched at the 52nd lattice site. b. Variation in the ensemble-averaged effective width (ω_{eff}) of a Gaussian beam (FWHM 10 µm) with propagation length of the waveguide lattice for different strengths of disorder. The error bars are the statistical standard deviations of effective beam widths.

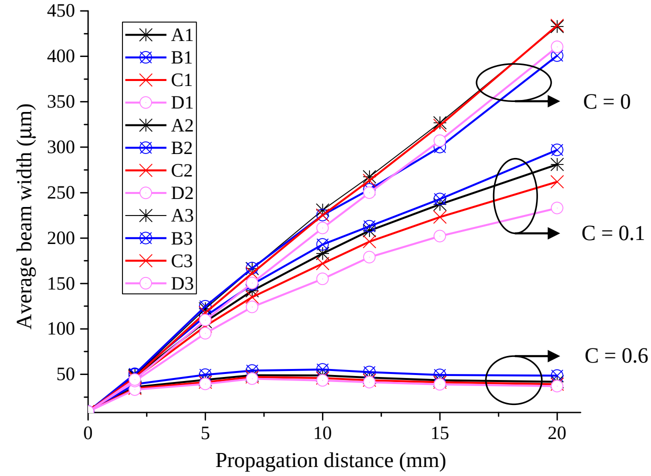

Fig. 5. Ensemble-averaged beam width (ω_{eff}) vs propagation distance for four different input spatial profiles (input FWHM: 10 µm). For the case of the ordered sample for which $C=0$, A1 corresponds to Gaussian, B1: parabolic, C1: hyperbolic secant, and D1: exponential profile. For the disordered samples having $C=0.1$ corresponding cases are marked as A2, B2, etc. and likewise for the case having $C=0.60$, the same are marked as A3, B3, etc.

array is *independent* of the shape of the input beam. Results of Figs. 4a and 5 also enable us to estimate the threshold level of disorder at which the significant localization of light occurs in our lattice geometry. The theoretical analogy and intuitive physical arguments have drawn the similarities between Anderson localization in 3D and counterpart transverse localization (e.g. in 1D and 2D geometries) [3,5]. Thus according to the theory of transverse localization of light in a 1D disordered lattice, an input beam of light will propagate along the length and expand until the beam diameter becomes of the order of the transverse localization length. In our chosen z-independent waveguide lattice geometry, as the transverse refractive index is a random function, constructive interference between the scattered lights will lead to localization of light injected by an input beam of arbitrary spatial shape as evidenced in simulation studies through exponentially decaying tail of the propagating beam [3]. The input CW light having a certain beam profile would be always localized in the presence of either diagonal or both diagonal and off-diagonal disorders [3,6]. Hence our numerical simulation results for transverse localization of light as an input beam profile-independent phenomenon evidently strengthen the theory and relax apparent constraints with regard to choice of specific input beam shapes in experimental studies of this phenomenon, which has lately attracted intense interest. Another important issue is whether, once the localization sets in for a given input beam profile, the localized state remains unchanged with further propagation inside the disordered medium. To investigate this, we analyze the transport dynamics shown in Figs. 4a and 5. Above the threshold disorder level, fluctuations in the effective width of a localized state are only due to its statistical nature. Our results clearly show that the average intensity profile of the localized state remains essentially unchanged with propagation, exhibiting a waveguide-like propagation of light in a disordered medium. It is our belief that these features could be exploited to realize discrete optical devices in disordered optical structures.

Fig. 6 shows the combined features of Figs. 4a and 5 by plotting effective beam width as a function of disorder parameter C at the output ends of two different lattice lengths of 10 mm and 20 mm, respectively for four different shapes of the input CW beam. In all

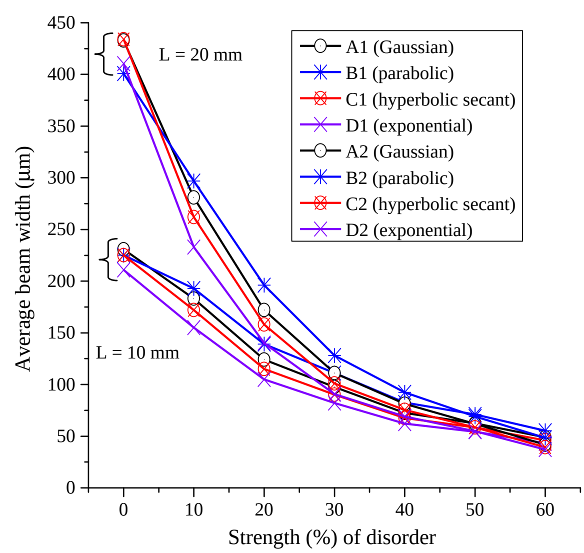

Fig. 6. Ensemble-averaged effective width (ω_{eff}) of the propagating beam (of four different spatial profiles) of FWHM 10 µm at the end of the lattice vs different strengths of disorder. Two sets of curves correspond to propagation through a 10 mm and 20 mm long lattice samples; Curves marked as A1, B1, etc have the same significance as in Fig. 5 i.e. each curve for a given length corresponds to different spatial beam profiles, namely Gaussian, parabolic, hyperbolic secant, and exponential profiles.

cases, a more disordered lattice with larger values of C increasingly favors localization. These features clearly indicate that transverse localization of the light beam always occurs as the level of disorder is increased progressively. From these results, it appears that a length of 15 mm would be sufficient to achieve localized state for the case of $C=0.6$. In order to test this hypothesis, we carried out further calculations for an input Gaussian beam of FWHM 10 μm in a 15 mm long waveguide lattice having 60% disorder, and the results are shown in Fig. 7a, in which a relatively smooth transition of the input Gaussian beam towards a localized state with propagation can be seen. This plot also highlights the evolution of the beam from the initial ballistic regime to a localized regime, through an intermediate co-existence of these two components. In order to corroborate our results with the theory of transverse localization, we have plotted the results from Fig. 7a for the realized localized state on a logarithmic scale in Fig. 7b. A clear presence of linearly decaying tails (equivalently exponential when plotted on a linear scale) on both sides of the beam profile confirms that the observed localization effect is of Anderson type.

Relatively large fluctuations in Fig. 7b are a result of the statistical nature of disorder. For a better agreement with the expected exponentially decaying tails, characteristic of localized light, we have averaged the output intensity profiles over 100 δ's. This average profile is shown in Fig. 8 on a log scale with the inset showing the same profile on a linear scale. Both the plots manifest the exponentially decaying tails, a well-known feature characteristic of Anderson localization in the presence of transverse disorder [3,5]. To further investigate the impact of input beam shape on the desired localized state, we depict in Fig. 9 the corresponding ensemble-averaged intensity profiles for three other input CW beams having spatial profiles as parabolic, hyperbolic secant and exponential. It is evident that the Anderson type of light localization occurs in each

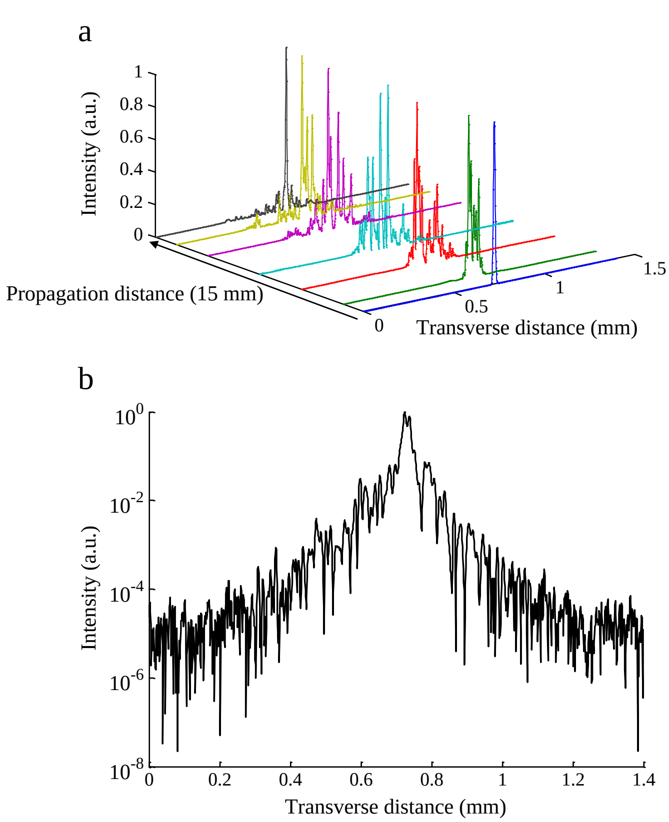

Fig. 7. a. Transition of an input Gaussian beam of width 10 μm (launched at 52nd site) to the localized state through a 15 mm long 60% disordered (a particular realization) lattice geometry. Two different propagation regimes (ballistic to localized) are clearly evident from this plot. b. Logarithmic plot of the intensity profile for the localized state (one realization) achieved in Fig. 7a showing the acquired linear tail.

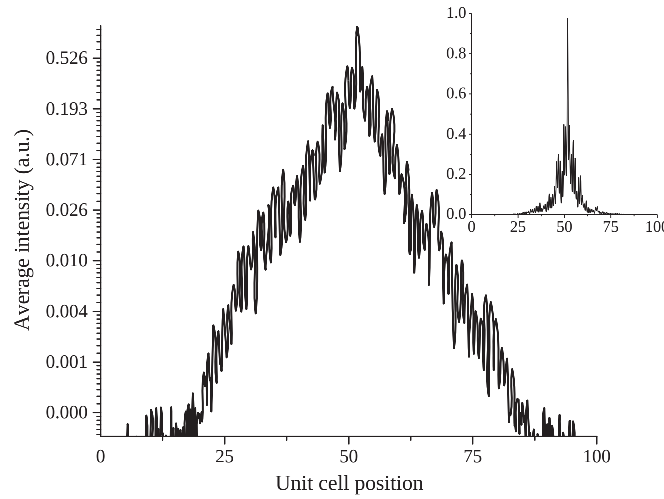

Fig. 8. Ensemble-averaged (over 100 realizations) intensity profile (logarithmic scale) of the localized state of an input Gaussian beam (FWHM 10 μm) after propagation of 15 mm through a 60% disordered lattice; the inset shows the corresponding plot on a linear scale.

case, irrespective of the input beam shape, once the level of disorder exceeds the threshold value for each beam shape.

For a deeper appreciation of the nature of localized states for different input profiles, we carried out further calculations and observed that, for our sample having an array of 100 waveguides, the localized states that were populated were not identical for the four input beam profiles. This is evident from the values of the transverse localization length plotted in Fig. 10 as a function of the disorder parameter C for the four different beam shapes but of the same FWHM. To obtain the localization length, we averaged 100 output intensity profiles for a given value of C and then performed a three-point moving average to smoothen further the resulting profile. In order to find the transverse localization length we then fitted the decaying tails with an exponential function of the form [5]

$$I \alpha \exp(-2|x|/L_c).$$

The nearly linear variation in the case of the exponential input profile indicates that in this case the transition to the localized state occurs in a smooth fashion in contrast to the cases of other spatial profiles. Variations in the localization lengths in Fig. 10 can be

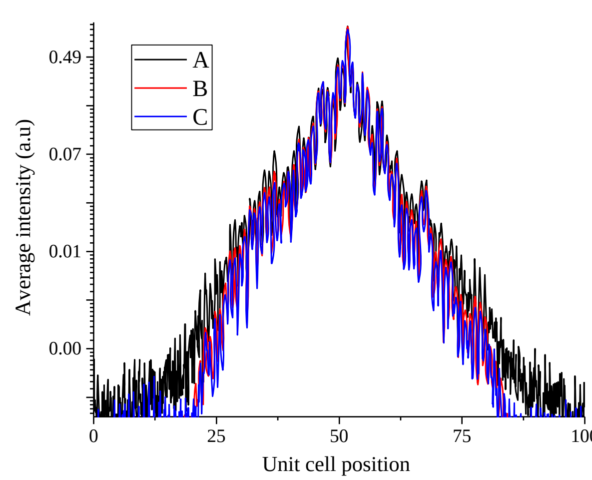

Fig. 9. Ensemble-averaged intensity profiles (logarithmic scale) of the localized state for three different input profiles (each of FWHM 10 μm) after propagation through 15 mm sample having $C=0.6$; A: parabolic, B: hyperbolic secant, and C; exponential.

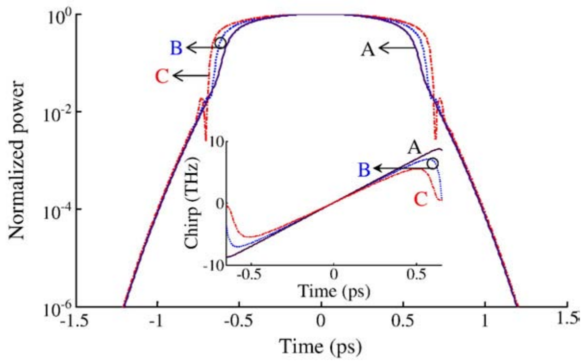

Fig. 10. Localization lengths vs levels of disorder for different input beam profiles over a 15 mm long lattice geometry; A: Gaussian, B: parabolic, C: hyperbolic secant, and D: exponential. As before, calculations have been carried over 100 ensembles of the same disorder level. Error bars show the possible fitting error encountered during calculations.

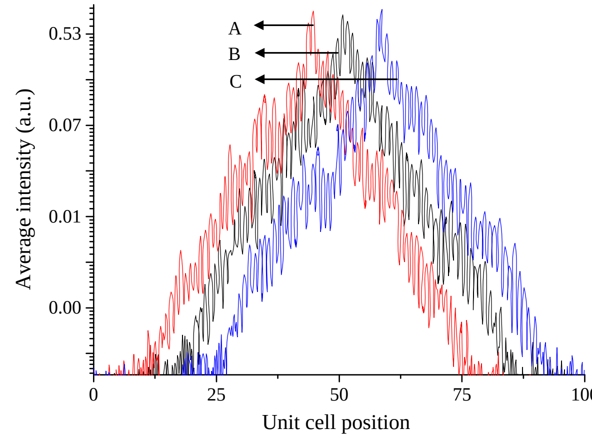

Fig. 11. Ensemble-averaged intensity profiles (logarithmic scale) of the localized state for an input Gaussian beam (FWHM 10 μm) launched at three different input lattice sites, after propagation through 15 mm long disordered lattice sample having $C = 0.6$; A: 45th lattice site, B; 52nd lattice site, and C: 59th lattice site.

interpreted as the signature of differences in the localized states for different input beam shapes.

We have also investigated dependence of the localized mode on the spatial location of the input beam on the input plane of the waveguide array for different beam widths covering one or more lattice units. For example, when a Gaussian input beam was incident at the 45th, 52nd and 59th waveguides of the sample, it evolved into a localized state in all the three cases, as shown in Fig. 11, with an ensemble-averaged ω_{eff} of 55.2 μm, 49.5 μm, and 51.8 μm, respectively. The closeness in these values indicates that the localization phenomenon is also independent of the location of the input beam as long as it is not launched too close to an edge of the sample. This is so because we need a sufficient number of lattice units on both sides of the injection point of the beam in order to realize localization. These results of Fig. 11 conclusively revealed that formation of the localized state is nearly independent of the input position of the incident beam though the shape of the localized eigenstate depends on the location of the input beam.

4. Conclusions

We have carried out a numerical study on various aspects of transverse light localization in a disordered waveguide lattice. Our results reveal that the phenomenon of light localization is independent of the input beam shape for a CW beam launched with a plane phase front. We have also investigated the dependence of the localized state on different parameters of the lattice as well as the input beam. The diffraction-free propagation of such a localized optical beam beyond its point of localization could be exploited to mimic waveguide-like propagation in discrete optical structures. Our study showing engineering the evolution of light beam in disordered photonic geometries (1D evanescently coupled multiple planar waveguides taken as an example) is significant as it reveals an additional wave-guiding platform in addition to already existing conventional waveguides and photonic bandgap fibers. Our comprehensive study on the light localization phenomena should be of interest to those involved in designing novel light-manipulating optical circuits for future optical telecommunication and sensing networks.

Acknowledgements

Part of these results was presented during the poster session of the workshop entitled "Nice Days at Nice on Random Lasers" held at LPMC, University of Nice, France during June 6–9, 2010. Patrick Sebbah, organizer of the workshop, is thanked for his invite to present this work at the workshop. One of the authors (BPP) thanks several experts from Europe, USA, and India, who came to this workshop, for their useful and constructive comments and his host Gerard Monnom for his help in the printing of the poster at a very short notice. He also gratefully acknowledges hosting of his short stay at LPMC by the Centre National de la Recherche Scientifique (CNRS, France). This work was also partially supported by an ongoing UKIERI project on Application Specific Microstructured Optical Fibers at IIT Delhi. One of the authors (GPA) thanks his *Alma Mater* IIT Delhi for hosting part of his sabbatical leave during which this work was originally initiated.

References

[1] S. John, Phys. Rev. Lett. 58 (1987) 2486.
[2] P.W. Anderson, Phys. Rev. 109 (1958) 1492.
[3] H. De Raedt, A. Lagendijk, P. de Vries, Phys. Rev. Lett. 62 (1989) 47.
[4] S. Mookherjea, J.S. Park, S.H. Yang, P.R. Bandaru, Nat. Photonics 2 (2008) 90.
[5] T. Schwartz, G. Bartal, S. Fishman, M. Segev, Nature 446 (52) (2007) 52.
[6] Y. Lahini, A. Avidan, F. Pozzi, M. Sorel, R. Morandotti, D.N. Christodoulides, Y. Silberberg, Phys. Rev. Lett. 100 (2008) 013906.
[7] P. Sebbah, C. Vanneste, Phys. Rev. B 66 (2002) 144202.
[8] C. Toninelli, E. Vekris, G.A. Ozin, S. John, D.S. Wiersma, Phys. Rev. Lett. 101 (2008) 123901.
[9] N.D. Psaila, R.R. Thomson, H.T. Bookey, N. Chiodo, S. Shen, R. Osellame, G. Cerullo, A. Jha, A.K. Kar, IEEE Photonics Tech. Lett. 20 (2008) 2, 126.
[10] G.N. Smith, K. Kalli, K. Sugden, Frontiers in Guided Wave Optics and Optoelectronics, In-Tech Pubs, Vienna, 2010.
[11] D.N. Christodoulides, F. Lederer, Y. Silberberg, Nature 424 (2003) 817.
[12] H.S. Eisenberg, Y. Silberberg, Phys. Rev. Lett. 81 (1998) 3383.
[13] D. Mandelik, H.S. Eisenberg, Y. Silberberg, R. Morandotti, J.S. Aitchison, Phys. Rev. Lett. 90 (2003) 053902.
[14] N. Belabas, S. Bouchoule, I. Segnes, J.A. Levenson, C. Minot, J.M. Moison, Opt. Exp. 17 (2009) 3148.